Simulation of back-injection molded parts using MAT_058 and MAT_215

Kai-Chien Chuang, Sanjay Kumar Sardiwal, Boris Cordero Porras, Patrick Scholz, Olaf Hartmann

ARRK Engineering GmbH

Abstract

Within the modern automotive industry, long-fiber-reinforced polymers (LFRPs) have gained increasing popularity because of efficient production of complex geometries in combination with relatively high stiffness and strength. Increased mechanical performance can be achieved by combining LFRP with continuous fiber composites, such as UD-Tape while using back-injection molding. The combination of these two material types poses a challenge in CAE, because of their individual anisotropic behavior.

The aim of this paper is to present a simulation approach for modeling the combination of LFRP with continuous fiber-reinforced thermoplastics (CFRTP) using the micro-mechanical-based material model MAT_215 for PP-LGF30 and MAT_058 for CF-PP-UD-Tapes in LS-DYN®. For material characterization purposes, coupon tests (e.g. tensile) are performed under different angles in order to determine the material properties of PP-LGF30. CT-Scans are performed on samples extracted from specific positions of the plate to identify the orientation tensors. For the CF-PP-UD-Tapes, additional coupon tests were performed in order to determine the longitudinal, transverse and shear properties.

Based on the coupon test results, the material properties were characterized for PP-LGF30 using MAT_215 taking the local anisotropy into consideration. For the CF-PP-UD-Tapes, the MAT_058 material model was calibrated with the experimental data. The numerical results in LS-DYNA® obtained for the coupon samples showed a good agreement with the experimental test results for both the PP-LGF30 and the CF-PP-UD-Tapes material. The anisotropy was also well captured for the LFRP at coupon level for Tension 0°, 45°, and 90°.

Furthermore, the calibrated material cards were implemented on a component level in order to validate their capability to capture the overall structural response of the simulation in comparison to the experimental results. Fiber mapping was implemented with fiber orientation data taken from a molding simulation. The numerical results from the component test showed a good agreement with respect to experimental data.

INTRODUCTION

The demand of fiber reinforced polymers (FRP) has been growing in automotive industry due to their desired features of high performance and light weight [1]. The improved production processes in recent years make these materials even more cost-effective and appealing for various vehicle applications [2]. The mechanical properties of such materials depend strongly on the fiber orientation. Unlike continuous fiber-reinforced polymer (CFRP), in which the fibers are unidirectional in each layer, the fibers in long fiber-reinforced polymer (LFRP) are varyingly distributed induced by the mold design, the molding parameters, the skin-core effect (the variation through the component thickness), etc. from the manufacturing process [3][4]. The randomness of fiber orientation in LFRP results in anisotropic behavior, which is difficult yet crucial to capture in order to have predictive and reliable simulation results in vehicle crash.

Several material models have been developed for anisotropic and orthotropic materials in LS-DYNA®. Among them, MAT_215 (***MAT_4A_MICROMEC**) using the micro-mechanic approach is capable of defining parameters of matrix and fiber distinctively, and estimating the overall behavior of composites

based on the given fiber orientation in the model through homogenization on the basis of Mori Tanaka Meanfield Theory and Eshelby's solution for ellipsoid inclusions [6][7][8][9]. The feature of MAT_215 therefore leads to a great advantage that the properties of LFRP composite can be calculated according to the assigned fiber orientation and therefore are dependent on the molding process. On the other hand, MAT_058 (***MAT_LAMINATED_COMPOSITE_FABRIC**) is designed to model composite with homogeneous fiber distribution and is therefore suitable for material with continuous fiber (e.g. CFRP). In this work, an approach of modeling FRP component considering the fiber orientation using both MAT_215 and MAT_058 was presented. The material models were firstly calibrated with coupons and employed to components - front bumper beams made from unidirectional tapes with carbon fiber and polypropylene (TAFNEX™ CF-PP-UD, fiber volume 50%) back-injection molded with a long fiber reinforced polypropylene (EDX-4030 PP-LGF30, fiber weight 30%) to validate the application.

METHODOLOGY

In the author's previous research, a material model of the CF-PP-UD-Tapes using MAT_058 has been created [10]. Thus, the current work focuses on the calibration of the material model of PP-LGF30 using MAT_215 as well as the implementation of calibrated material models with the fiber information from molding simulation in the component modeling (see Figure 1). The material plates and components for testing, as well as fiber orientation scan data and molding simulation are provided by Mitsui Chemicals Group, the parent company of ARRK Engineering. All the testing program was performed at the in-house testing facility at ARRK Engineering in Munich.
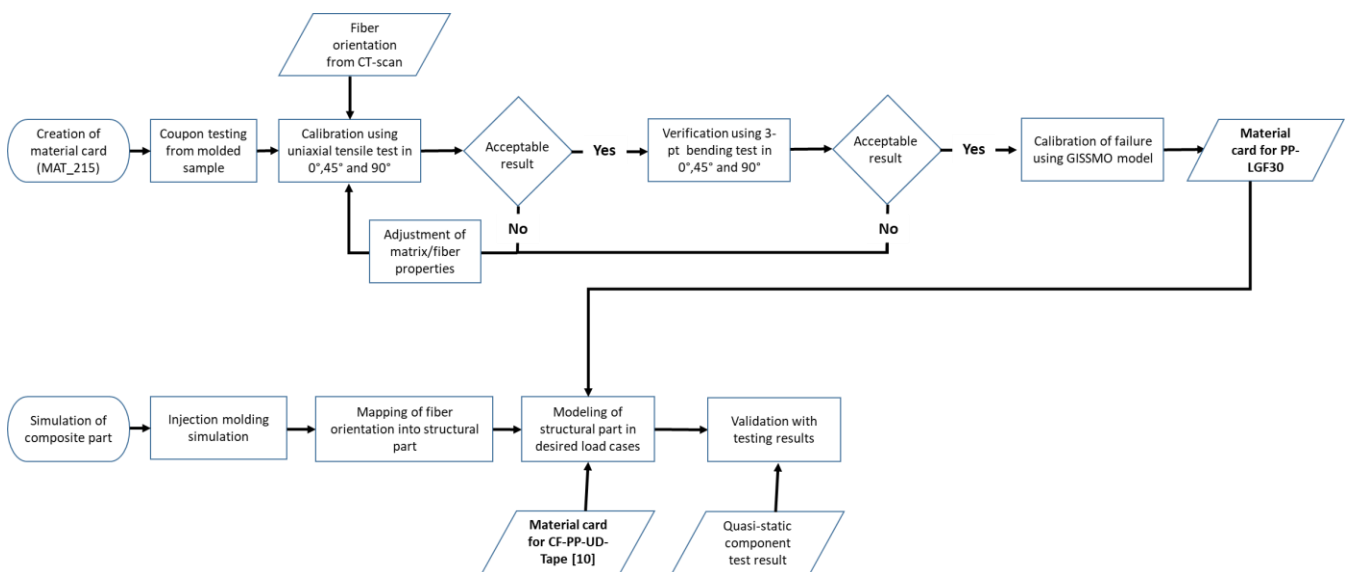

Figure 1: Framework of the present study.

To create the material model for PP-LGF30, tensile and bending tests in three different degrees - 0°, 45° and 90° were performed. The coupons were cut out from base plates using water-jet, prepared and tested based on DIN 527-2 (for tension) and ISO 14125 (for bending). The fiber orientation in coupon was defined through orientation tensor data obtained from Computer Tomography (CT) scan technique. An initial material card with properties of matrix material and fiber, including fiber aspect ratio, fiber volume fraction, fiber diameter, etc. provided from supplier was created and applied to a solid model with mesh size of 1.0 mm containing 20 elements through thickness.

The fiber orientation tensors identified from CT-scan, as shown in Figure 2(a), were assigned to each layer accordingly using keyword ***INITIAL_STRESS_SOLID_SET** (see Figure 2(b)) and the material orientation was defined to be consistent with the testing in 0°, 45° and 90° separately by the

parameter AOPT in the material card. The elastic and plastic properties of matrix as well as the parameters of fiber were therefore calibrated and finalized by the means of reverse engineering using the tensile tests and verified through the coupon bending test. The failure flag was set to consider composite failure. In addition, the failure criteria varies subject to the loading condition and hence, the GISSMO damage model was introduced to capture the rupture of composite based on the failure behavior in the tests. After the material model was created, it was tested with the shell model to ensure the viability when applying to the component model later.
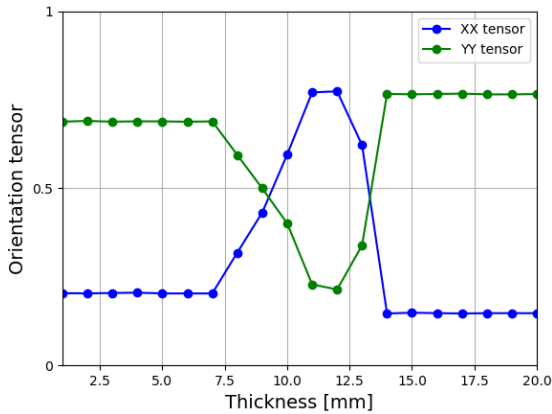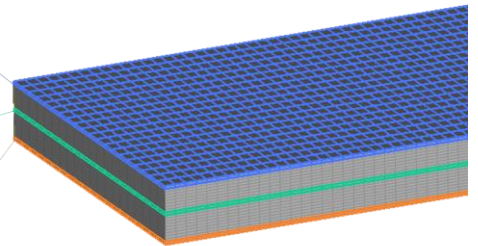

Figure 2a: CT scan data through the specimen thickness. The YY-tensor defines the orientation in the flow direction and the XX-tensor represents the orientation tangential to it

Figure 2b: FE solid model contains 20 layers of element through thickness. Various fiber orientation tensor from the CT scan data were assigned to each layer of element

To put the created PP-LGF30 model into application on component, the fiber orientation in the component has to be acquired. The fiber orientation is influenced by and significantly dependent of the injection molding process. With the aid of molding simulation (e.g. Moldex 3D used in the work), the polymer flow pattern and state in the part, including the fiber distribution and orientation can be estimated, exported as tensor format for every element and eventually applied to the structural model (see Figure 3). The discretized model used in molding simulation (source solid mesh) is however different from the one used in the structural simulation (target shell mesh). Consequently, a mapping technique via software Envyo, provided by Dynamore was employed so that the fiber orientation results of the source mesh from Moldex 3D were transferred and compatibilized to the specific input format feasible for the target mesh in LS-DYNA®.
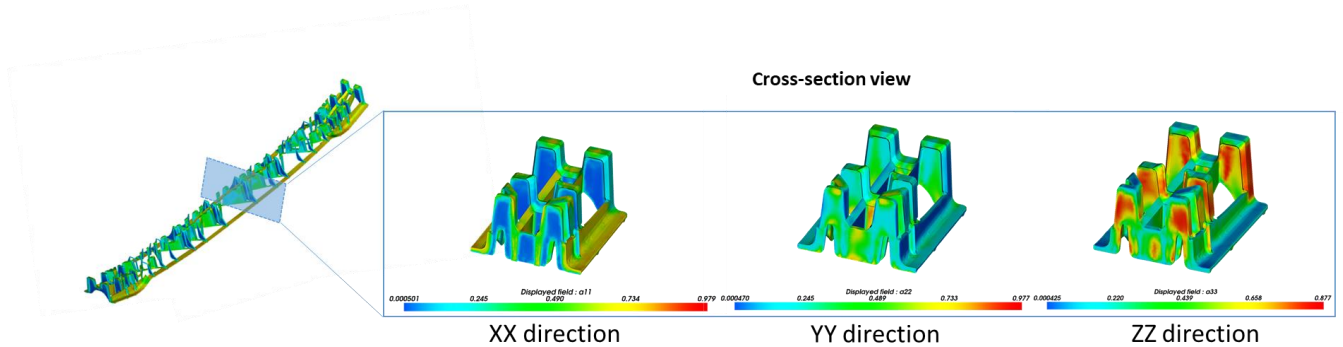

Figure 3: The fiber distribution and orientation after the injection molding process obtained from the mold flow simulation

The MAT_215 material model for PP-LGF30 along with MAT_058 for the CF-PP-UD-Tapes were applied to the component model correspondingly as shown in Figure 4(a). The part for PP-LGF30 was prepared as simple shell element with mesh size of 4 mm using Elform 16 and the fiber orientation input was included and read based on the element ID. The part for CF-PP-UD-Tapes on the other hand was built with reduced stacked shell of three layers (mesh size of 4 mm using Elform 10) connected by cohesive elements via MAT_138 (***MAT_COHESIVE_MIXED_MODE**) with Elform 20 so that the delamination of CFRP can be properly represented [10]. Furthermore, two cases of layups – (1) 90/0/($\pm$45)$_8$/0/90 and (2) ($\pm$45)$_{10}$ were defined in ***PART_COMPOSITE** individually to model the response of these two kinds of components. The simulation follows the setup of the quasi-static component test as shown in Figure 4(b), performed using LS-DYN® version R11.2.2 mpp.
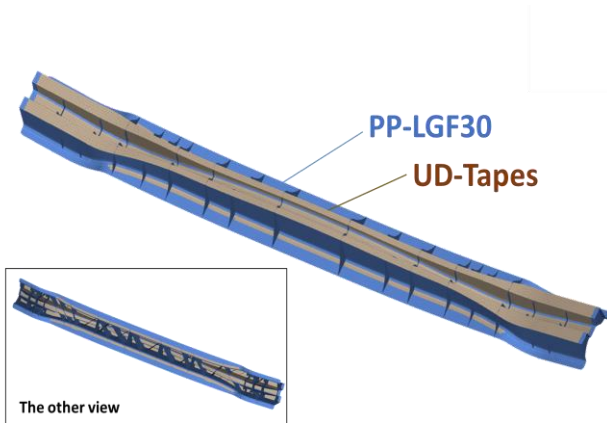

Figure 4a: The front bumper beam model made from TAFNEX™ CF-PP-UD-Tapes and back-injection molded with PP-LGF30.

Figure 4b: The setup for quasi-static testing of the component. An impactor with diameter of 100 mm and supporters with diameter of 50 mm in a distance of 795 mm was set.

RESULTS

Results are presented in two parts: material calibration at coupon level and approach validation with components. Following the sequence of elasticity, plasticity and failure, the MAT_215 was defined step by step and the characterized properties were summarized in Table 1. The elasticity was firstly calibrated by adjusting the elastic modulus of matrix and fiber material using tensile test results. Parameters were optimized so that the elastic behavior in simulations match testing results in 3 various orientations (the linear part of the strain-stress curves in Figure 5).

The plastic property of composite is dominated by the matrix material, defined through the hardening curve in the model. A pronounced difference in the behavior of strength, despite scattering, was seen in the test – the strength decreases as the testing orientation changes from 0° to 90°. However, the behavior of matrix in MAT_215 is isotropic, meaning only one hardening curve can be defined. Thus, a compromise among results of three orientations had to be made. A good compromise was found as shown in Figure 5. Despite slight underestimation in tension in 90°, the results of tension in 0° and 45° agreed well with the testing curves. Finally, criteria of plastic strain to failure was optimized based on the tensile test results in 3 orientations and the simulations fitted the experimental curves well.

The defined material model was verified using bending tests as shown in Figure 6. The results have good agreement with the tests considering the elastic and plastic behaviors in general. Deviations in the bending in 45° were observed and may be a result of scattering in manufacturing because the specimens

of bending were cut from a different plate, which may contain different fiber orientation compared to the one used for tensile specimens and for CT-scan. Additionally, the material model underestimated the failure in all bending results, which might be caused by the fact that there are various defects commonly generated along the molding process, such as voids and shrinkage. These defects usually play a significant role in the damage and failure of the molded parts. When the failure was calibrated based on tensile tests, in which the loaded area in the specimen was large so that the influence from the defects were also stronger, the failure would likely be triggered earlier. As a consequence, the failure criteria may be too strict when used in bending tests, in which the impacted area was considerably smaller and contained less defects.

The calibrated material card was tested with the shell elements by allotting fiber orientation tensors to each integration point along the thickness. Similar results to the solid modeling were observed and were acceptable. Next, the material card was applied on component level to validate the capability of capturing the overall structural response.

Table 1: PP-LGF30 material properties characterized in the work.

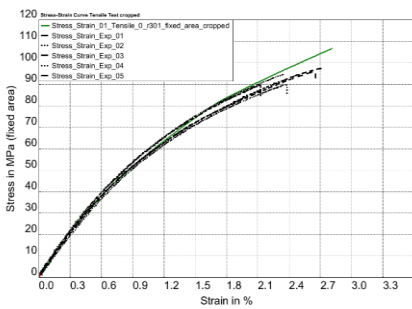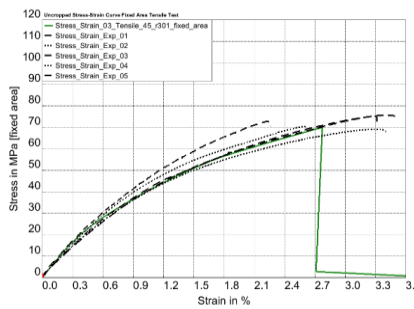|	Elasticity_L [MPa]	Elasticity_T [MPa]	Shear modulus [MPa]	Poisson's ratio	Aspect ratio	Volume fraction
Glass fiber	72000	72000	28800	0.22	100	0.15
PP matrix	2488		--	0.41	--	--

Figure 5a: Tension in 0°
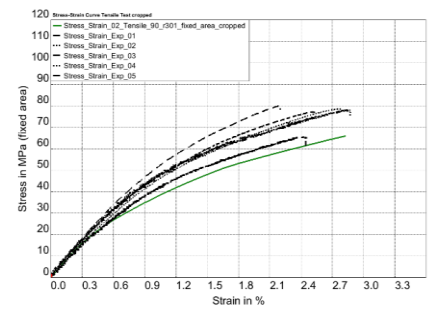

Figure 5b: Tension in 45°
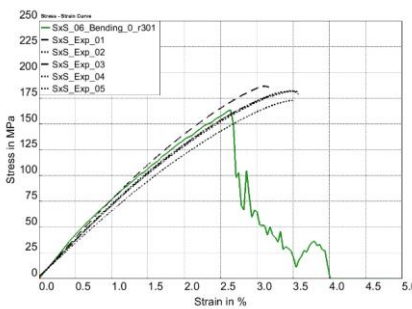

Figure 5c: Tension in 90°

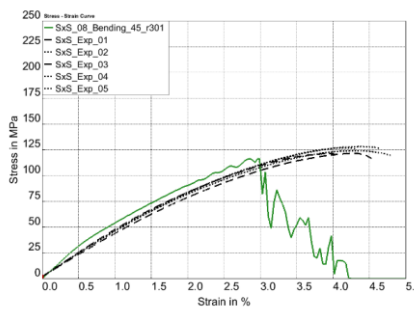**Figure 6a:** Bending in 0°

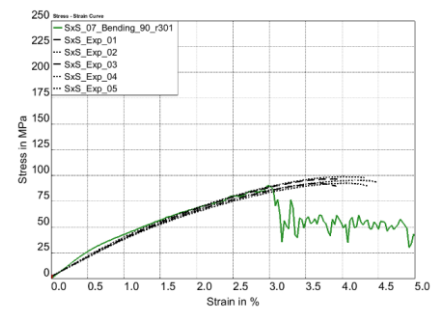**Figure 6b:** Bending in 45°

Figure 6c: Bending in 90°

The simulation results were compared to the force-displacement curves of the 3-point bending tests for the bumper beams of two different CF-PP-UD-Tape layups and good agreement were seen in both cases, as shown in Figure 7. Although there were certain deviations, such as the overestimated stiffness at the beginning of the curve, they were acceptable since the overall load level, the major failure event and the post-failure behavior were generally captured. The deviations seen might be attributed to the numerical limitations of using shell elements, the deflections of the fiber orientation in PP-LGF30 from

the molding simulation, and the fluctuations in the layups of CF-PP-UD-Tape, which were presumably altered slightly after the back injection molding process. Furthermore, as previously seen and discussed in the coupon results of bending, there were inevitably defects induced in the manufacturing process leading to the deviations between simulation and testing results as well.
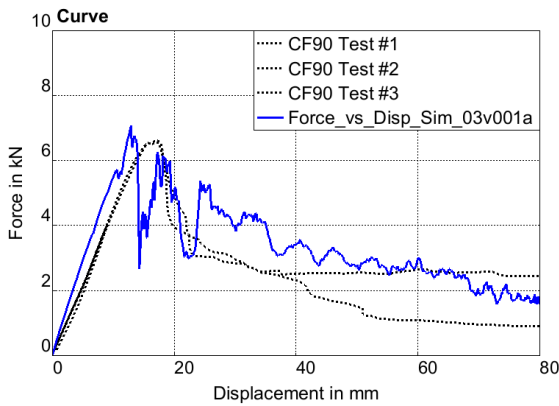

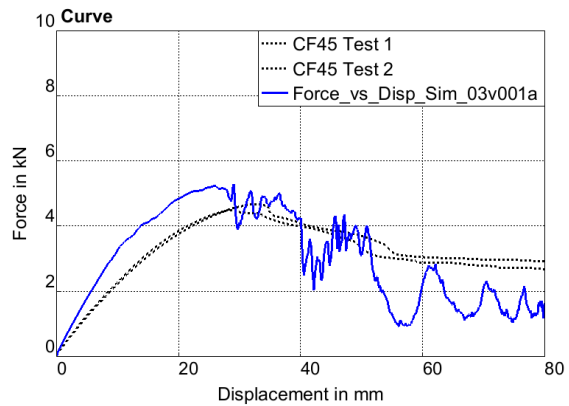**Figure 7a:** Force-displacement curve for components composed of CF-PP-UD-Tape with a layup of $90/0/(\pm45)_8/0/90$.

Figure 7b: Force-displacement curve for components composed of CF-PP-UD-Tape with a layup of $(\pm45)_{10}$.

SUMMARY

The current work proposed a solution for modeling composite component of LFRP and CFRTP and validated it using the component made of PP-LGF30 and CF-PP-UD-Tapes. It was shown that the properties of PP-LGF30 could be majorly characterized using MAT_215 with the fiber orientation obtained from CT-scan. Through the aid of molding simulation and the mapping technique, the anisotropy of fiber in PP-LGF30 was estimated and successfully aligned to the structural part, and became the key element of the good results shown in the paper. Besides the complexity of non-uniformity from the PP-LGF30, the manufacturing process of the component brought also a lot of variables into the properties, which were difficult to predict and completely implement in the modeling. As a result, certain degree of deviation was unavoidable and acceptable.

To apply to crash simulation at full-vehicle scale, strain rate dependency might play a critical role and should be as well considered. Therefore, the strain rate properties of both PP-LGF30 and CF-PP-UD-Tapes will be investigated and studied together with drop-tower test as the next step.

EDX4030 PP-LGF30 and TAFNEX™ CF-PP UD material from Mitsui Chemicals Group is commercially available and can be applied for joint discussion of new projects.

LITERATURE

1 Park, C-K., Kan, C-D., Hollowell, W., & Hill, S.I. (2012, December). *Investigation of opportunities for lightweight vehicles using advanced plastics and composites.* Washington, DC: national Highway Traffic Safety Administration.

2 Friedrich, K., Almajid, A.A., (2012, February) *Manufacturing Aspects of Advanced Polymer Composites for Automotive Applications.* Appl Compos Mater **20**, 107-128

3 Huang, P. W., Peng, H. S., Hwang, S. J., Huang, C. T., Chen, P. C., Ke, Y. Y., Pan, P. S., Wu, C. C., & Tu, C. I. (2019, March). *Study of the effect of process parameters on fiber length, fiber orientation and tensile strength of long glass fiber reinforced polypropylene molding.* Detroit, 77th Annual Technical Conference of the Society of Plastics Engineers.

4 Advani, S. & Sozer, M. (2010, July). *Process Modeling in Composites Manufacturing.*

5 Reithofer, P., Fertschej, A., Hirschmann, B., Jilka, B., Erhart, A., & Hartmann, S. (2018, June). **MAT_4A_MICROMEC – Theory and Application notes.* Detroit, 15th International LS-DYNA® Users Conference

6 Mori, T., Tanaka, K. (1973, May) *Average Stress in Matrix and Average elastic Energy of Materials with misfitting Inclusions*, Acta Metallurgica, **21**, 571-574

7 Tucker C. L. III, Liang, E. (1999, April). *Stiffness Predictions for Unidirectional Short-Fibre Composites:Review and Evaluation*, Composites Science and Technology, **59**, 655-671

8 Eshelby, J. D. (1957) *The determination of the elastic field of an ellipsoidal inclusion, and related problems*, Proceedings of the Royal Society, Vol.A, No241, 376-396.

9 Maewal A., Dandekar D.P. (1987). *Effective Thermoelastic Properties of Short-Fibre Composites*, ActaMechanica, 66

10 Hartmann, O. (2020, June). **Stacked Shell Modeling for Evaluation of Composite Delamination in Full Vehicle Simulations.* 16th International LS-DYNA® Users Conference